

Orientation to polarized light in tethered flying honeybees

Norihiro Kobayashi¹, Ryuichi Okada^{1,2} and Midori Sakura^{1*}

¹Department of Biology, Graduate School of Science, Kobe University, Rokkodai 1-1, Nada-ku, Kobe, Hyogo 657-8501, Japan

²School of Human Science and Environment, University of Hyogo, 1-1-12 Shinzaike-Honcho, Himeji, Hyogo 670-0092, Japan

Key Words: insect flight; polarization vision; dorsal rim area; polarotaxis; navigation

*Correspondence to Midori Sakura

Phone: +81-78-803-5711 Fax: +81-78-803-5711

E-mail: skr@port.kobe-u.ac.jp

Abbreviations:

clockwise; CW

counterclockwise; CCW

dorsal rim area; DRA

preferred e-vector orientation; PEO

Summary statement

Tethered flying bees exhibited polarotaxis under an overhead rotating e-vector stimulus, in which their right-and-left abdominal movements were coincident with the rotation of the stimulus.

ABSTRACT

Behavioral responses of honeybees to a zenithal polarized light stimulus were observed using a tethered animal in a flight simulator. Flight direction of the bee was recorded by monitoring the horizontal movement of its abdomen, which was strongly anti-correlated with its torque. When the e-vector orientation of the polarized light was rotated clockwise or counterclockwise, the bee responded with periodic right-and-left abdominal movements; however, the bee did not show any clear periodic movement under the static e-vector or depolarized stimulus. The steering frequency of the bee was well coordinated with the e-vector rotation frequency of the stimulus, indicating that the flying bee oriented itself to a certain e-vector orientation, i.e., exhibited polarotaxis. The percentage of bees exhibiting clear polarotaxis was much smaller under the fast stimulus (3.6° s^{-1}) compared with that of the slow stimulus (0.9 or 1.8° s^{-1}). The bee did not demonstrate any polarotactic behavior after the dorsal rim region of its eyes, which mediates insect polarization vision in general, was bilaterally covered with black paint. Preferred e-vector orientations under the clockwise stimulus varied among individuals and distributed throughout -90 to 90° . Some bees showed similar preferred e-vector orientations for clockwise and counterclockwise stimuli whereas others did not. Our results strongly suggest that the flying honeybees utilize the e-vector information from the skylight to deduce their heading orientation for navigation.

INTRODUCTION

As a result of sunlight scattering in the atmosphere, the skylight is partially plane-polarized and the celestial e-vectors are arranged in a concentric pattern around the sun (Strutt, 1871; Wehner, 1997). It is well known that many insects exploit this skylight polarization for visual compass orientation and/or navigation (for review: Wehner, 1994; Wehner and Labhart, 2006; Heinze, 2014). There have been an enormous number of studies about insect polarization vision, not only at the behavioral level (e.g., Dacke et al., 2003; Reppert et al., 2004; Heinze and Labhart, 2007; Weir and Dickinson, 2012), but also at the neural network level, such as sensory (e.g., Blum and Labhart, 2000; Weir et al., 2016) and central brain mechanisms (e.g., Labhart 1988; Heinze and Homberg, 2007; Sakura et al., 2008; Heinze and Reppert, 2011; Bech et al., 2014). The e-vector detection in insects is mediated by a group of specialized ommatidia located in the most dorsal part of the compound eye, the dorsal rim area (DRA), in which the photoreceptors are monochromatic and highly polarization-sensitive (for review: Labhart and Meyer, 1999; Wehner and Labhart, 2006). The neural pathway of polarization vision in the brain has been documented in several species. The photoreceptors in DRA is terminated into the lamina or the medulla in the optic lobe, and from there, polarized light signals primarily projected into the central complex through a pathway involving the lower unit of the anterior optic tubercle and lower division of the central body (Homberg, 2008). The central complex, one of the higher centers of the insect brain, is considered to be the location of an internal compass (for review: Homberg et al., 2011; Heinze, 2017), although it is still unclear how the central complex controls the animal's steering during navigation.

Foraging behavior in social insects, such as ants and bees, is a useful model system for studying insect navigation because they repeatedly go back and forth between the nest and a feeding site. In particular, the path integration mechanisms in the desert ants *Cataglyphis* have been extensively studied in regard to insect navigation (Wehner, 2003; Collett and Carde, 2014), and *Cataglyphis* is well known to choose their heading direction using celestial polarization cues during long distance navigation (Fent, 1986; Wehner, 1997; Wehner and Müller, 2006). In addition to path integration based on the polarization compass, ants could learn visual landmarks or panoramic views at familiar locations and use them for local navigation (Collett et al., 1992; Wehner et al., 1996; Collett et al., 1998; Graham and Cheng, 2009; Narendra et al., 2013). Honeybees also undertake long-distance foraging trips that may reach over 5 km (Couvillon et al., 2014). Usage of skylight polarization in honeybees to detect their intended travel direction was first described by von Frisch (1967) through a series of sophisticated behavioral studies on

the waggle dance. Thereafter, the waggle dance orientations of the nest-returning bees from a certain feeder have been intensively studied. These studies were conducted under a patch of polarized light stimulus or part of the sky and an internal representation of the celestial e-vector map has been proposed (Rossel and Wehner, 1982, 1986, 1987; Wehner, 1997). These systematic studies have focused on modification of the waggle dance orientation and not on how the bees perceive polarized light from the sky en route to/from the nest. More recently, polarized light detection in flying bees has been demonstrated using a four-armed tunnel maze with a polarizer on top (Kraft et al., 2011) and it was revealed that bees choose the arms based on their previous e-vector experiences. Moreover, it has also been demonstrated that bees memorize the e-vector orientations experienced during their foraging flight and use that memory for the subsequent waggle dances (Evangelista et al., 2014). In these studies, the tunnel was made as the bee could receive parallel or vertical e-vector stimulus with respect to their moving direction. Indeed, by classical conditioning experiments, it has been shown that the honeybees are able to discriminate polarized light of 0° e-vector orientation with that of 90° (Sakura et al., 2012).

Behavioral responses of moving insects to the overhead polarized light stimulus have been intensively studied using a tethered animal. Orientation to the polarized light, i.e. polarotaxis (Mathejczyk and Wernet, 2019), has been demonstrated not only in tethered walking insects (cricket *Gryllus campestris*: Brunner and Labhart, 1987; fly *Musca domestica*: von Philipsborn and Labhart, 1990) but also in tethered flying insects. In the locust *Schistocerca gregaria*, direct monitoring of yaw-torque responses showed clear polarotactic right-and-left turns to rotating polarized light (Mappes and Homberg, 2004). In tethered monarch butterflies *Danaus plexippus*, measuring flight orientations using an optical encoder revealed that their flight orientation under natural skylight was clearly affected by a dorsally presented polarization filter (Reppert et al., 2004; but see also Stalleicken et al., 2005). Similar orientation to polarized skylight has also been demonstrated in *Drosophila* (Weir and Dickinson, 2012; Mathejczyk and Wernet, 2019), in which a fly was magnetically tethered in the arena and its flight heading was recorded from above by an infrared camera. Recently, some behavioral studies have succeeded to make a dorsally tethered bee stably fly by presenting lateral optic flow and frontal air-flow stimuli (Luu et al., 2011; Taylor et al., 2013). It was observed that the tethered bees showed “streamlining” responses, whereby they raised their abdomen in a correlated manner with the speed of the optic and air-flow stimuli. In the present study, we investigated how the flying bees respond to polarized light stimuli using the tethered system. We constructed a flight simulator, in which we could examine the tethered bee’s flight response to a rotating polarized stimulus and found that they tended to orient themselves to a certain e-vector direction, i.e., they exhibited

clear polarotaxis, during the flight.

MATERIALS AND METHODS

Animals

The honeybees, *Apis mellifera* L., used in this study were reared in normal ten-frame hives on the campus of Kobe University. Forager honeybees with pollen loads were collected at the hive entrance before the experiment and anesthetized on ice or in a refrigerator. An L-shaped metal rod for tethering was attached to the pronotum of an anesthetized bee, as previously described (Luu et al., 2011). Briefly, the hair on the pronotum was gently shaved using a small piece of a razor blade, and the metal rod was adhered using a small amount of light-curing adhesive (Loctite; Henkel, Dusseldorf, Germany). The following image analyses of bee behavior (see below) were conducted by marking the tip of the abdomen with a white light-curing dental sealant (Conseal f; SDI Ltd., Bayswater, Australia). Next, the bees were placed in a warm room to recover from anesthesia and fed several drops of 30 % sucrose solution before the experiment. We did not purposely remove pollen loads of the bees but some of them lost the pollen loads during the preparation processes and we left them as they were.

Setup

The experiments were performed using a custom-made black box (Fig. 1) in a dark room. A tethered bee was mounted in the box by attaching the end of the metal rod to a three-dimensional manipulator such that the bee's location could be adjusted manually. The flying behavior of the tethered bee was enhanced by stimulating the bee with a headwind from an air circulator and front-to-back optic flow from a LCD monitor. The circulator was located outside of the box and connected to a tunnel that carried the wind stimulus into the box. The end of the tunnel (diameter, 8 cm), consisting of many fine plastic straws to reduce the turbulent flow of wind, was fixed at 10 cm from the bee's head. The wind speed at the bee's head was almost constant ranging between 1.7 to 2.0 m s⁻¹. The LCD monitor (RDT1711LM; Mitsubishi Electric, Tokyo, Japan; 75 Hz refresh rate), covered with a sheet of tracing paper to eliminate any polarized components of the light, was located 5 cm beneath the tethered bee. The front-to-back optic flow stimulus of moving black-and-white stripes (Michelson contrast = 0.25) was displayed on the monitor using a self-made program in Microsoft Visual C++. The size of the area on the monitor displaying the stripes was 159 ° W x 163 ° L, and the width of the single stripe was 40 °, both measured from the bee's

head position. The speed of the stimulus was approximately $900^{\circ} \text{ s}^{-1}$, as seen by the bee, which is fast enough to elicit the highest “streamlining” responses of the bee (Luu et al., 2011).

Light from a xenon lamp (LC8, L8253; Hamamatsu Photonics, Hamamatsu, Japan) was applied above the bee using a quartz light guide. The light was filtered using a depolarizer (DPU-25; ThorLabs, Newton, NJ) at the end of the light guide to eliminate any polarized components of the light and a holographic diffuser (48-522; Edmund Optics, Barrington, NJ) was clamped under the end of the light guide. The diffuser reduced illuminance irregularity and increased the size of the light fit around a linear polarizer (HN42HE; diameter, 15 cm; Polaroid Company, Cambridge, MA) beneath the diffuser. The polarizer was mounted on a circular holder that could be rotated using a DC motor. The stimulus was centered at the bee's zenith (with respect to flying head position) at a distance of 15 cm, providing a dorsal, polarized stimulus of 53° in diameter. In the experiments, in which unpolarized light stimulus was used, the depolarizer was clamped just above the bee's head instead of at the end of the light guide such that the size of the light stimulus covered the entire receptive field of the bee's DRA. Under this condition, we could assess the effect of a slight fluctuation in light intensity caused by the polarizer rotation with the same spectrum of the light (300 – 620 nm). The intensity of the polarized and unpolarized light at the animal level was approximately 1000 lx.

Behavioral experiments

The behavioral experiments were performed at between 11:00 and 18:00 in local time. A bee with the metal rod was fixed in the experimental box after complete recovery from anesthesia. First, we let the bee hold a small piece of paper so that it could not start flying. The e-vector angle of the polarizer was set at 0° with respect to the bee's body axis, and static black-and-white stripes were displayed on the PC monitor. After the bee had been familiarized with the box, the paper was removed to allow the bee to start flying, and the wind and optic flow stimuli were simultaneously presented. After the bee's flight became stable, in which the bee raise the abdomen up, did not thrash the legs and extend the antennal flagella forward, the polarizer started rotating slowly (0.9 , 1.8 , or $3.6^{\circ} \text{ s}^{-1}$), and the behavior of the bee was monitored for 600 s. When a bee stopped flying before 600 s, the data were not used in the analysis. In the experiments showing Figs 2 and 3, the bee was tested 3 times under different stimulus conditions—clockwise (CW), static, and counterclockwise (CCW). To eliminate possible effects of the stimulus sequence, the order of these three stimuli was randomly changed for each experiment. In other cases, a bee was tested only with the CW stimulus.

The flying behavior of the tethered bee was monitored using a USB camera (IUC-300CK2; Trinity Inc., Gunma, Japan) placed behind the bee (see Fig. 1). Images of the bee were recorded at a rate of 1 Hz, i.e., 600 images for 10 min data. For each image, the x-coordinate of the bee's abdominal tip was determined manually to estimate flying orientation (see Fig. S1). A series of x-coordinates was then calibrated into actual distances (in mm) from the center, where the tethering wire was fixed and used for further analysis (see below).

Whether the DRA of the compound eye was involved in flying behavior under the polarized light stimulus was determined using bees whose DRAs were painted (Fig. 7C, D). The DRAs were painted as in our previous work (Sakura et al., 2012) with black acrylic emulsion paint (Herbol; Cologne, Germany) under a dissecting microscope just before the tethering procedure described above. The DRA of a compound eye is visually identifiable because the cornea appears slightly grey and cloudy (Meyer and Labhart, 1981). Because it was technically not possible to cover the DRA alone, which consists of only 4–5 horizontal rows of ommatidia (see Meyer and Labhart, 1981; Wehner and Strasser, 1985), a small area of the unspecialized dorsal region next to the DRA was also painted. After the experiments, the paint cover was checked in all the experimental animals under a dissecting microscope. Data for cases in which any of the paint was missing were excluded from further analysis. The three ocelli, which are not involved in polarization vision (Rossel and Wehner, 1984), were not painted in the experiments.

Analysis and statistics

All data analyses were performed using self-made programs in MATLAB (MathWorks Inc., MA, USA). Periodicity of the time course of the abdominal tip location was analyzed using the fast Fourier transform (FFT). For FFT, data for only the last 400 s of each trajectory (600 s in total) were used because the periodicity of a bee's flight was occasionally obscure at the beginning of the stimulus (e.g., see gray part in Fig. 2Ac). The relative power spectrum was calculated, and peak frequencies were determined. In the case when the power spectrum had multiple peaks, we took into account only the maximum and the second maximum peaks for the analysis. We defined a bee to be aligned with a certain e-vector orientation or showing “polarotaxis”, when the power spectrum of the bee showed the maximum or the second maximum peak at the stimulus frequency, half rotation of the polarizer (note that the e-vectors 0° and 180° are identical); i.e., 0.5, 0.01, and 0.02 Hz for 0.9, 1.8, and 3.6° s^{-1} stimuli, respectively. Distributions of bees showing polarotaxis were statistically analyzed using Fisher's exact test or Cochran's Q -test with post-hoc McNemar test for among- or within-group comparisons, respectively. In addition, the largest peak in the power spectrum of each bee was determined to compare the distribution of

the peaks by a bee.

In the case of experiments where 1.8° s^{-1} CW stimulus was used, a preferred e-vector orientation (PEO) for each bee that demonstrated polarotaxis was examined. The PEO was obtained from a phase (in degree), φ , of the stimulus frequency component (0.01 Hz) in the division signal after FFT. Here,

$$\varphi = \tan^{-1} \frac{b_n}{a_n}$$

Where a_n and b_n are Fourier cosine and sine coefficient for 0.01 Hz, respectively.

The PEO in CW or CCW stimulus was given as follows:

$$\text{PEO}_{cw} = 90 - \frac{\varphi + 90}{2}$$

$$\text{PEO}_{ccw} = 180 - \frac{\varphi + 90}{2}$$

where PEO_{cw} , and PEO_{ccw} indicate the PEO for CW, and CCW stimulus, respectively (in degrees). The uniformity of the distribution of PEOs was statistically analyzed by the Rayleigh test (Batschelet, 1981) using Oriana software (ver. 3.12; Kovach Computing Services, UK), in which the axial PEO data were converted to angular data by multiplying two.

Simultaneous recordings of abdominal images and yaw-torque

To determine the relationship between a tethered bee's abdominal location and its flying behavior (Fig. S1), we simultaneously recorded abdominal images and the yaw torque of a flying tethered bee in the following procedures. Forager bees were collected at the hive entrance in the morning (9-10 am) and anesthetized in a refrigerator at 4°C for 10–20 min. A small, thin metal plate (1 mm W \times 2 mm H, and 0.02 mm in thickness) was glued on the center of the thorax of each bee with bee's wax. After recovery from anesthesia, the bee was tethered by attaching the metal plate to the torque meter (SH-02S, Suzuko, Yokohama, Japan). Before starting the experiment, a small piece of paper was provided to cause the bee to remain stationary and familiarize itself with the experimental environment.

All experiments were performed under dark conditions. Two monitors were facing each other and a bee was positioned at the center of the monitors and 13 cm from each monitor. Vertical black-white gratings (visual angle = 125°) with a sinusoidal illuminance change were presented on both monitors and moved from front to rear of the bee. To facilitate flight, a gentle laminar air flow (approximately 1.8 m s^{-1}) was provided by a fan placed in front of the bee. During the flight, the bee was monitored by a CCD camera (Sun Star 300, Electrophysics, Fairfield, NJ) located to the posterior of the bee facing the abdominal tip. By using this camera,

we were able to obtain the position of the tip of the abdomen, as well as the behavior of the bee.

Three kinds of visual stimuli with air flow were applied for 30 sec to induce a putative “straight” or “turning” flight. For straight flight, gratings of both monitors moved at the same speed of $110.5^{\circ} \text{ s}^{-1}$ (a spatial frequency is 7.5 Hz). For putative turning flight, either the left or right monitor presented a faster speed ($331.5^{\circ} \text{ s}^{-1}$), by moving one at a greater speed than the other ($110.5^{\circ} \text{ s}^{-1}$) and vice versa. In this condition, the stimulated bee, in general, tended to turn to the slower side. One bee was subjected to three kinds of visual stimuli three times each. Air flow was constant throughout the experiments. Only bees that exhibited 30 sec flight were used for further analysis.

The yaw torque from the torque meter was stored in the PC through an A/D converter using custom-made software with a sampling rate at 120 points per second. A video movie was simultaneously stored with 30 frames per second in the avi format. To see the correlation between yaw torque and flight posture, the tip of the abdomen was manually tracked frame by frame after converting the movie into JPG images with an interval of 0.1 sec. By using custom-made software, we obtained x and y coordinates along with time. Because we were only interested in horizontal movements of the abdomen, we used only x coordinates for further analysis.

We calculated correlation coefficients between torque and the abdominal movement for all flights of all individuals. For calculation, we normalized horizontal movements individually as follows. All sampled x-coordinates obtained from three putative straight flights of a bee were averaged as a neutral position for the bee. Then, relative positions of the abdominal tips to the neutral position were calculated for each flight by converting pixels to distance (in mm). In this normalization, a positive value indicated that the abdomen was positioned on the right side to the base position and the negative value indicated the left. For yaw torque, a positive/negative value meant a clockwise/counterclockwise turn. Only yaw torques of the corresponding time points to the manual tracking were used, i.e., the sampling interval was reduced to 0.1 sec. Because the posture of a flying bee was not stable for the first 2-5 sec after the onset of the stimulation, we discarded the first 10 sec of data and used only the last 20 sec for the correlation analysis.

RESULTS

Polarotactic behavior of tethered bees

Under our experimental condition, approximately two-thirds of the experimental tethered bees could stably fly for over 10 min. A representative horizontal trajectory of a bee's abdominal tip under the three different polarized light conditions is shown in Fig. 2A. When the e-vector of the polarized light stimulus was gradually (1.8° s^{-1}) rotated clockwise or counterclockwise, the bee showed a periodic right-and-left abdominal movement, regardless of the rotational direction (Fig. 2Aa, c). The FFT analysis of the last 400 s of the trajectory data clearly showed that these abdominal movements were synchronized with an e-vector rotating frequency of 0.01 Hz (180° rotation) (Fig. 2Ba, c). Conversely, a bee did not show such periodic movement under the static e-vector stimulus (0° with respect to the body axis; Fig. 2Ab), and the peak of the power spectrum (PS) was detected at 0.0025 Hz instead of at 0.01 Hz, which is coincident with the entire data length (Fig. 2Bb, see below). We also determined the relationship between a tethered bee's abdominal location and its flying behavior (see Fig. S1). Simultaneous recordings of the abdominal images and the yaw torque of a flying tethered bee showed a strong negative correlation, i.e., the bee's abdominal tip moved right when the bee turned left and *vice versa*. Therefore, the bee's periodic abdominal movement under the rotating e-vector stimulus could be explained that the bee periodically changed the steering action to adjust the flying direction to a certain e-vector orientation. If a given e-vector heading is desirable, the bee treated it as a target, steering left as the target approaches in CW rotation and then steering right as it exits. At the orthogonal e-vector heading (an anti-target), the bee first steered right on CW approach and left on exit. Such a steering pattern could produce abdomen movement at twice the frequency of stimulus rotation given the axially symmetric e-vector stimulus. The PEO_{CW} and PEO_{CCW} of the bee showing in Fig. 2, calculated by the phase of 0.01 Hz component in the PS (see Materials and Methods), were 126° and 112° , respectively (Fig. 2, arrows). Around these e-vector directions, in fact, the bee's abdominal tip was located at almost the center, indicating that the bee did not change her flying direction.

Figure 3D-F summarizes the PSs of all experimental bees tested under the three different conditions; CW, static and CCW polarized light stimulus. Under the CW and CCW rotations, the PS often had a strong power at 0.0025 and/or 0.01 Hz regardless of the rotational direction (Fig. 3D, F) whereas it did only at 0.0025 Hz with static stimulus in most bees (Fig. 3E). A significantly higher number of bees (4, 3 and 2 of 21 bees for both CW and CCW, CW only, and CCW only, respectively) displayed the maximum peaks at 0.01 Hz in the PS compared with that

(none of the 21 bees) under the static 0° e-vector stimulus (Fig. 3A-C; CW: $p = 0.008$, CCW: $p = 0.014$, Cochran's Q -test with post-hoc McNemar test). In the averaged PS, a clear peak was noted at 0.01 Hz under the CW or CCW stimulus, although another strong power was detected at 0.0025 Hz (Fig. 3A, C), and the strong power was only detected at 0.0025 Hz under the static stimulus (Fig. 3B). To confirm that the strong power at 0.0025 Hz reflects the entire data length, we also performed FFT analysis for the data under CW stimulus of different data length, i.e., 100, 200, 300, 400, 500 and 600 s (Fig. S2). In all cases, the averaged PS curves have two peaks, one at (data length) $^{-1}$ Hz and the other at 0.01 Hz. The peak at 0.01 Hz was always found in the PS regardless of the data length (Fig. S2, red column) indicating that the trajectory has certain periodicity with 0.01 Hz. Considering that the strong power at 0.0025 Hz based on the data length was often found in the PSs, we next counted the number of the bees showing the maximum or the second maximum peak at 0.01 Hz in each stimulus condition. In total, over half of the experimental bees showed a clear peak at 0.01 Hz in the PS under the rotating e-vector stimulus (Fig. 3D, F; 10, 2 and 4 of 21 bees for both CW and CCW, CW only, and CCW only, respectively); however, under the static 0° e-vector stimulus, only 2 of the 21 bees showed a 0.01 Hz peak in the PS, which was significantly smaller than the number of bees showing a peak at 0.01 Hz under the rotating stimulus (Fig. 3E; CW: $p = 0.008$, CCW: $p = 0.001$, Cochran's Q -test with post-hoc McNemar test).

To determine whether the periodic movements were not elicited by the rotation of the e-vector, but rather by a slight fluctuation in light intensity caused by the polarizer rotation, we projected an unpolarized light stimulus through the depolarizer beneath the CW rotating polarizer (see Materials and Methods). Under the unpolarized light stimulus, the bees did not show any clear movements coincident with the polarizer rotation (Fig. 4A). Furthermore, no detectable peak at 0.01 Hz was noted in the averaged PS, and none of the eight experimental bees demonstrated the maximum peak at 0.01 Hz while six of the eight bees showed the maximum power at 0.0025 Hz (Fig. 4B). Only one bee showed the small second maximum peak at 0.01 Hz, which was significantly different from that under the CW polarized stimulus ($p = 0.044$, Fisher's exact test). These results indicate that the abdominal periodic movements were elicited by the rotation of the polarized e-vector orientation. Take these results together, we concluded that the tethered flying bees oriented to the certain e-vector direction, in other words, showed polarotaxis.

Polarotaxis under the different speeds of the stimulus

Next, we observed polarotaxis of the tethered bees under CW rotating e-vector stimulus at twice the speed ($3.6^{\circ} \text{ s}^{-1}$) or 2-times slower the speed ($0.9^{\circ} \text{ s}^{-1}$) to confirm that the periodicity in the abdominal movement (Fig. 2, 3) was not elicited by internal rhythm but by external polarized light stimuli. Under the faster stimulus, some bees still showed right-and-left abdominal movements synchronized to the stimulus rotation (Fig. 5A). However, in contrast to the $1.8^{\circ} \text{ s}^{-1}$ stimulus, the PS of the abdominal trajectory showed only a small peak at a stimulus frequency of 0.02 Hz (Fig. 5B). Moreover, in the averaged PS of all 14 experimental bees, a small, but detectable, peak at 0.02 Hz and the maximum peak at 0.0025 Hz were noted (Fig. 5C). The number of bees showing the peak at 0.02 Hz in the PS was significantly different from experiencing the $1.8^{\circ} \text{ s}^{-1}$ stimulus (7 of 14 bees for $3.6^{\circ} \text{ s}^{-1}$ and none of the 21 bees for $1.8^{\circ} \text{ s}^{-1}$ stimulus; $p = 0.0005$, Fisher's exact test), although only one of the 14 experimental bees showed the maximum peak at 0.02 Hz (Fig. 5C). These results indicated that the bees exhibited weak polarotaxis to the fast rotating e-vector stimulus.

Under the slower rotating stimulus, the tethered bees showed clear right-and-left abdominal movements (Fig. 6A) and the PS of which had the maximum peak at the stimulus frequency of 0.005 Hz (Fig. 6 B). Four of the 10 experimental bees exhibited the maximum peak at 0.005 Hz in each PS of the abdominal trajectory (Fig. 6C), whereas only one of the 21 bees did so under the $1.8^{\circ} \text{ s}^{-1}$ stimulus, which was significantly lower ($p = 0.0274$, Fisher's exact test). This result indicated that the bees also responded to a slow stimulus. However, we could not detect a 0.005 Hz peak in the averaged PS, although the power at 0.005 Hz was relatively high compared with that under other stimulus conditions (Fig. 6C); this could have occurred because the peak could not be clearly separated from the peak at 0.0025 Hz owing to data interference from unresponsive bees (see Figs 3B, 4C).

Selective stimulation of eye regions

Polarization vision in insects is known to be mediated by the DRA of the compound eye. To confirm the sensory input area for polarotaxis in the eye, we covered a part of each compound eye and restricted the area receiving light stimulation to the DRA (Fig. 7D, E). The bees whose DRA was covered did not show polarotactic abdominal movement even under the $1.8^{\circ} \text{ s}^{-1}$ CW rotating polarized light stimulus to which intact bees responded (Fig. 7A), and no clear peak was noted at the stimulus frequency of 0.01 Hz in the power spectrum (Fig. 7B). The averaged power spectrum of all eight experimental bees did not exhibit a peak at 0.01 Hz (Fig. 7C), indicating

that the bees with covered DRA lost the ability to orient to certain e-vectors. Similar to the response of intact bees to a static stimulus, none of the eight bees displayed the maximum peak at 0.01 Hz (Fig. 7C, see also Fig. 3B), and their response was not significantly different ($p = 1$, Fisher's exact test). Conversely, the number of bees showing the maximum peak at 0.01 Hz was also not significantly different than that of the intact bees under the CW stimulus (see Figs 3A, 7C; $p = 0.1421$, Fisher's exact test), probably owing to the small number of experimental bees used.

Preferred e-vector orientation

We assessed the PEO_{cw} of the 21 bees that showed polarotaxis under the 1.8° s^{-1} CW stimulus. In addition to the 12 bees in the experiments showing Fig. 3, another data from 9 bees were newly obtained from 16 bees tested in total under the CW stimulus. The PSs of all 37 individuals testing under the 1.8° s^{-1} CW stimulus (21 bees in Fig. 3 and additional 16 bees) were summarized in Fig. S3. The PEO_{cw} of each bee varied from -90 to 90° (Fig. 8). However, more than half of the bees (14 of 21) showed PEO_{cw} between -60 to 0° and the distribution was not significantly random ($p = 0.01$, Rayleigh test). We also tried to compare the PEO_{cw} and PEO_{ccw} of the 10 bees that showed polarotaxis both in CW and CCW stimuli in the experiments shown in Fig. 3 (Fig. S4). Although some bees showed similar PEOs in CW and CCW stimulus, the difference between them ($PEO_{cw} - PEO_{ccw}$) were quite varied ($-3.48 \pm 37.74^\circ$, $N = 10$).

DISCUSSION

Behavioral response to the polarized light stimulus in the honeybee

In the present study, we directly showed that bees tended to orient to the certain e-vector angles during their flight under the tethered condition, i.e., they referred polarized light information to control their flight direction. The fact that fewer bees responded to the fast stimulus (3.6° s^{-1} , Fig. 5) than the slow stimuli (0.9° s^{-1} and 1.8° s^{-1} , Fig. 2, 3, 6) is also indicative of the use of e-vector orientation as a global cue for orientation. Probably, they did not refer to the e-vector when it quickly changed because they did not expect such a situation, except when they quickly changed their flight direction. It is also possible that the fast rotating stimulus caused optomotor response in which the bee steered in the same direction as the rotating stimulus at all e-vector orientations. To confirm this possibility, we performed a trend analysis for the all behavioral data shown in Figure 3, 5 and 6 (Fig. S5). If the bee showed a strong optomotor response, it should show a constant steering trend toward the stimulus direction. However, in all stimulus conditions,

the trend was varied among individuals and we could not find any prominent correlations between steering and stimulus directions (Fig. S5B, C). For more precise verification of the optomotor responses for the rotating e-vector, the comparison between the behavior under the fast CW and CCW stimulus will be necessary.

The bee whose DRA was blinded did not show any polarotaxis (Fig. 7). It is well known that detection of skylight polarization in insects is mediated by ommatidia in the DRA (for review: Labhart and Meyer, 1999; Wehner and Labhart, 2006). In honeybees, UV-sensitive photoreceptors of the ommatidia in DRA are highly polarization-sensitive, and their receptive field covers a large part of the celestial hemisphere, which is suitable for observing the sky (Labhart, 1980; Wehner and Strasser, 1985). Behaviorally, it has also been demonstrated that covering the DRA impaired correct coding of food orientation by the waggle dance orientation (Wehner and Strasser, 1985) and discrimination of different e-vector orientations by classical conditioning (Sakura et al. 2012). These results clearly show that bees utilize polarized light detected by the ommatidia in the DRA for orientation.

Polarotaxis in insects

Polarotaxis in insects has been demonstrated in several species. Obviously, orientation to a certain e-vector direction is a common occurrence among insect species that utilize skylight polarization for navigation. Classically, it has been tested using a treadmill device in the cricket *Gryllus campestris* (Brunner and Labhart, 1987) and the fly *Musca domestica* (von Philipsborn and Labhart, 1990). Using such a device, the insect was tethered on an air-suspended ball and its walking trajectory could be monitored through the rotation of the ball. In these species, the insect on the ball showed clear polarotactic right-and-left turns when the e-vector of the zenithal polarized light stimulus was slowly rotated, as we showed in this study in flying honeybees. This kind of behavior does not merely demonstrate they have polarization vision but also allowed us to clarify fundamental properties of insect polarization vision, e.g., perception through the DRA in the compound eye (Brunner and Labhart, 1987), monochromatic spectral sensitivity (Herzmann and Labhart, 1989; von Philipsborn and Labhart, 1990), and sensitivity to the degree of polarization (Henze and Labhart, 2007).

Orientation to the polarized light has been investigated in tethered flying insects as well by monitoring yaw-torque responses (locust *Schistocerca gregaria*: Mappes and Homberg, 2004), flight orientations (monarch butterflies *Danaus plexippus*: Reppert et al., 2004) or changes in body axis (*Drosophila*: Weir and Dickinson, 2012; Mathejczyk and Wernet, 2019). A potential problem in investigating polarization vision in tethered flying insects is that sometimes the

tethering apparatus, including the torque meter or other recording devices, interrupt a part of the visual field of the tested animal. In the present experiments, we succeeded in evaluating the bee's polarotactic flight steering by simply monitoring the horizontal position of the abdominal tip that was strongly anti-correlated with the torque generated by the bee (see Fig. S1). Using these methods, the entire visual field of the animal remained open; therefore, it had an advantage for investigating the animal's responses under various stimulus conditions.

Preferred e-vector orientation

The PEO distribution has been reported in several species. In walking crickets and flies, a weak preference to an e-vector orientation perpendicular to their body axis was demonstrated, although the reason of this behavior was not clear (Brunner and Labhart, 1987; von Philipsborn and Labhart, 1990). On the other hand, in flying locusts and *Drosophila*, the PEOs were randomly distributed and they did not show any directional preferences as a population (Mappes and Homberg, 2004; Warren et al., 2018; Mathejczyk and Wernet, 2019). In the present study, even though the sample size might be still small to conclude their heading preferences, the distribution was significantly non-uniform and bees seemed to prefer e-vector orientations skewed left of the body axis (Fig. 8). In some bees, the PEOs under CW and CCW stimulus were quite similar (Fig. S4). Therefore it was possible that, at least in these bees, each bee had its own PEO and used it not only as a reference for maintaining straight flight but also to deduce its heading orientation. Further investigation of the PEOs in CW and CCW of the bees would be necessary to confirm whether each bee had a specific PEO.

Considering that central place foragers, such as honeybees, have to change their navigational directions depending on the currently available food locations, their PEOs would reflect their previous foraging experiences. In the present study, we collected the bees with a pollen load at the hive entrance; therefore, all experimental forager bees were returners. Consequently, we could no longer assess their feeding locations when we measured their flight responses in the laboratory. Moreover, their path-integration vector should be reset to a zero-state in such a situation (Sommar et al., 2008), and they might not have had a strong motivation to use polarized light cues for navigation. To further clarify the role of polarization vision in flying foragers, testing the PEOs in the bees in different navigational states will be crucial.

Acknowledgements

The authors are deeply grateful to Dr. M. V. Srinivasan and Dr. T. Luu for helpful advice regarding the construction of the flight simulator. We also thank Dr. Y. Hasegawa, Dr. H. Ikeno, and Ms. H. Onishi for their help measuring the torque of flying bees.

Competing interests

No competing interests declared.

Funding

This work was supported by KAKENHI from the Japan Society for the Promotion of Science (15KT0106, 16K07439, and 17H05975 to MS; 16K07442 to RO) and Bilateral Joint Research Project with Australian Research Council from Japan Society for the Promotion of Science (CH50427010) to MS.

REFERENCES

- Batschelet, E.** (1981) *Circular statistics in biology*. Academic Press: New York.
- Bech, M., Homberg, U. and Pfeiffer, K.** (2014) Receptive fields of locust brain neurons are matched to polarization patterns of the sky. *Curr. Biol.* **24**, 2124-2129.
- Brunner, D. and Labhart, T.** (1987) Behavioural evidence for polarization vision in crickets. *Physiol. Entomol.* **12**, 1-10.
- Collett, M., Collett, T. S., Bisch, S. and Wehner, R.** (1998) Local and global vectors in desert ant navigation. *Nature* **364**, 269-272.
- Collett, T. S., Dillmann, E., Giger, A. and Wehner, R.** (1992) Visual landmarks and route following in desert ants. *J. Comp. Physiol. A* **170**, 435-442.
- Couvillon, M. J., Schürch, R. and Ratnieks, F. L. W.** (2014) Dancing bees communicate a foraging preference for rural lands in high-level agri-environment schemes. *Curr. Biol.* **24**, 1212-1215.
- Dacke, M., Nilsson, D.-E., Scholtz, C. H. Byrne, M. and Warrant, E. J.** (2003) Insect orientation to polarized moonlight. *Nature* **424**, 33.
- Evangelista, C., Kraft, P., Dacke, M., Labhart, T. and Srinivasan, M. V.** (2014) Honeybee navigation: critically examining the role of the polarization compass. *Phil. Trans. R. Soc. B* **369**, 20130037.
- Fent, K.** (1986) Polarized skylight orientation in the desert ant *Cataglyphis*. *J. Comp. Physiol. A* **158**, 145-150.
- Graham, P. and Cheng, K.** (2009) Ants use the panoramic skyline as a visual cue during navigation. *Curr. Biol.* **19**, R935-R937.
- Heinze, S.** (2014) Polarized-light processing in insect brains: recent insights from the desert locust, the monarch butterfly, the cricket, and the fruit fly. In *Polarized light and polarization vision in animal sciences* (ed. G. Horváth), pp. 61-111. Berlin-Heidelberg: Springer-Verlag.
- Heinze, S.** (2017) Unraveling the neural basis of insect navigation. *Curr. Opin. Insect Sci.* **24**, 58-67.

- Heinze, S. and Homberg, U.** (2007) Maplike representation of celestial e-vector orientations in the brain of an insect. *Science* **315**, 995-997.
- Heinze, S. and Homberg, U.** (2009) Linking the input to the output: new sets of neurons complement the polarization vision network in the locust central complex. *J. Neurosci.* **29**, 4911-4921.
- Heinze, S. and Reppert, S. M.** (2011) Sun compass integration of skylight cues in migratory monarch butterflies. *Neuron* **69**, 345-358.
- Henze, M. and Labhart, T.** (2007) Haze, clouds and limited sky visibility: polarotactic orientation of crickets under difficult stimulus conditions. *J. Exp. Biol.* **210**, 3266-3276.
- Herzmann, D. and Labahrt, T.** (1989) Spectral sensitivity and absolute threshold of polarization vision in crickets: a behavioral study. *J. Comp. Physiol. A* **165**: 315-319.
- Homberg, U.** (2008) Evolution of the central complex in the arthropod brain with respect to the visual system. *Arthropod Struct. Dev.* **37**: 347-362.
- Homberg, U., Heinze, S., Pfeiffer, K. Kinoshita, M. and el Jundi, B.** (2011) Central neural coding of sky polarization in insects. *Phil. Trans. R. Soc. B* **366**, 680-687.
- Kraft, P., Evangelista, C., Dacke, M., Labhart, T. and Srinivasan, M. V.** (2011) Honeybee navigation: following routes using polarized-light cues. *Phil. Trans. R. Soc. B* **366**, 703-708.
- Labhart, T.** (1980) Specialized photoreceptors at the dorsal rim of the honeybee's compound eye: polarizational and angular sensitivity. *J. Comp. Physiol. A* **141**, 19-30.
- Labhart, T.** (1988) Polarization-opponent interneurons in the insect visual system. *Nature* **331**, 435-437.
- Labhart, T. and Meyer, E. P.** (1999) Detectors for polarized skylight in insects: a survey of ommatidial specializations in the dorsal rim area of the compound eye. *Microsc. Res. Tech.* **47**, 368-379.
- Luu, T., Cheung, T., Ball, D. and Srinivasan, M. V.** (2011) Honeybee flight: a novel 'streamlining' response. *J. Exp. Biol.* **214**, 2215-2225.
- Mappes, M. and Homberg, U.** (2004) Behavioral analysis of polarization vision in tethered flying locusts. *J. Comp. Physiol. A* **190**, 61-68.

Mathejczyk, T. F. and Wernet, M. F. (2019) Heading choices of flying *Drosophila* under changing angles of polarized light. *Sci. Rep.* **9**, 16773.

Meyer, E. P. and Labhart, T. (1981) Pore canals in the cornea of a functionally specialized area of the honey bee's compound eye. *Cell Tissue Res.* **216**, 491-501.

Narendra, A., Gourmaud, S. and Zeil, J. (2013) Mapping the navigational knowledge of individually foraging ants, *Myrmecia croslandi*. *Proc. Biol. Sci.* **280**, 20130683.

Reppert, S. M., Zhu, H. and White, R. H. (2004) Polarized light helps monarch butterflies navigate. *Curr. Biol.* **14**, 155-158.

Rossel, S. and Wehner, R. (1982) The bee's map of e-vector pattern in the sky. *Proc. Natl. Acad. Sci. USA* **79**, 4451-4455.

Rossel, S. and Wehner, R. (1984) Celestial orientation in bees: the use of spectral cues. *J. Comp. Physiol. A* **155**, 605-613.

Rossel, S. and Wehner, R. (1986) Polarization vision in bees. *Nature* **323**, 128-131.

Rossel, S. and Wehner, R. (1987) The bee's e-vector compass. In *Neurobiology and behavior of honeybees* (ed. R. Menzel and A. Mercer), pp. 76-93. Berlin: Springer-Verlag.

Sakura, M., Lambrinos, D. and Labhart, T. (2008) Polarized skylight navigation in insects: model and electrophysiology of e-vector coding by neurons in the central complex. *J. Neurophysiol.* **99**, 667-682.

Sakura, M., Okada, R. and Aonuma, H. (2012) Evidence for instantaneous e-vector detection in the honeybee using an associative learning paradigm. *Proc. Roy. Soc. B* **279**, 535-542.

Sommer, S., von Beeren, C. and Wehner, R. (2008) Multiroute memories in desert ants. *Proc. Natl. Acad. Sci. USA* **105**, 317-322.

Stalleicken, J., Mukhida, M., Labhart, T., Wehner, R., Frost, B. and Mouritsen, H. (2005) Do monarch butterflies use polarized skylight for migratory orientation? *J. Exp. Biol.* **208**, 2399-2408.

Strutt, J. (Lord Rayleigh) (1871) On the light from the sky, its polarization and colour. *Phil. Mag.* **41**, 107-120.

- Taylor, G. J., Luu, T., Ball, D. and Srinivasan M. V.** (2013) Vision and airflow combine to streamline flying honeybees. *Sci. Rep.* **3**, 2614.
- von Frisch, K.** (1967) *The dance language and orientation of bees*. Cambridge: Belknap Press.
- von Philipsborn, A. and Labhart, T.** (1990) A behavioural study of polarization vision in the fly, *Musca domestica*. *J. Comp. Physiol. A* **167**, 737-743.
- Warren, T. L., Weir P. T. and Dickinson, M. D.** (2018) Flying *Drosophila melanogaster* maintain arbitrary but stable headings relative to the angle of polarized light. *J. Exp. Biol.* **221**, jeb.177550.
- Wehner, R.** (1994) The polarization-vision project: championing organismic biology. In *Neural basis of behavioural adaptation* (ed. K. Schildberger and N. Elsner), pp. 103-143. Stuttgart: Fischer-Verlag.
- Wehner, R.** (1997) The ant's celestial compass system: spectral and polarization channels. In *Orientation and communication in arthropods* (ed. M. Lehrer), pp. 145-185. Basel: Birkhäuser Verlag.
- Wehner, R.** (2003) Desert ant navigation: how miniature brains solve complex tasks. *J. Comp. Physiol. A* **189**, 579–588.
- Wehner, R. and Labhart, T.** (2006) Polarization vision. In *Invertebrate vision* (ed. E. Warrant and D. E. Nilsson), pp. 291-348. Cambridge: Cambridge University Press.
- Wehner, R. Michel, B. and Antonsen, P.** (1996) Visual navigation in insects: coupling of egocentric and geocentric information. *J. Exp. Biol.* **199**, 129-140.
- Wehner, R. and Müller, M.** (2006) The significance of direct sunlight and polarized skylight in the ant's celestial system of navigation. *Proc. Natl. Acad. Sci. USA* **103**, 12575-12579.
- Wehner, R. and Strasser, S.** (1985) The POL area of the honey bee's eye: behavioural evidence. *Physiol. Entomol.* **10**, 337-349.
- Weir, P. and Dickinson, M. H.** (2012) Flying *Drosophila* orient to sky polarization. *Curr. Biol.* **22**, 21-27.
- Weir, P. T., Henze, M., Bleul, C., Baumann-Klausener, F., Labhart, T. and Dickinson, M. H.** (2016) Anatomical reconstruction and functional imaging reveal an ordered array of skylight polarization detectors in *Drosophila*. *J. Neurosci.* **36**, 5397-5404.

Figures

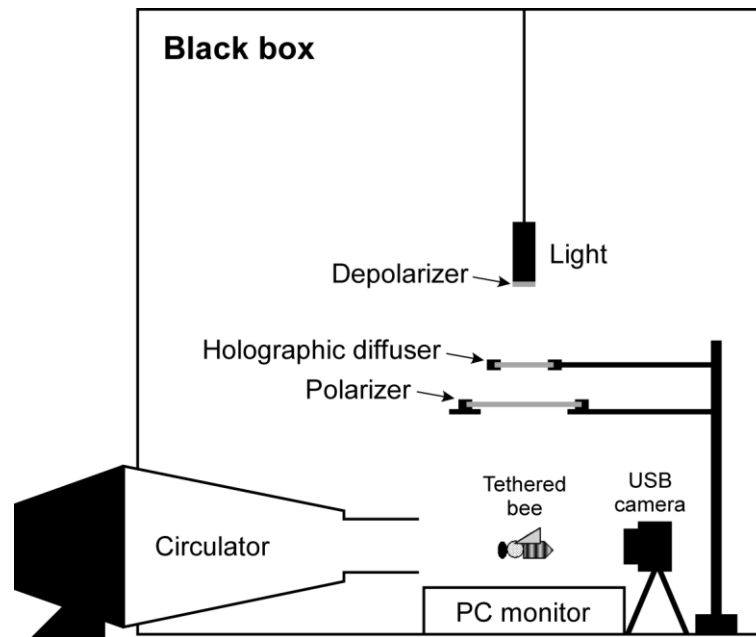


Fig. 1. Experimental setup. Light from a xenon lamp was equally depolarized and then linearly polarized using a UV-transmitted polarizer. A bee was tethered under the polarizer and its flight was monitored by a USB camera. For the stable flight of a tethered bee, rectified wind from a circulator and moving black-and-white stripes on a PC monitor were presented.

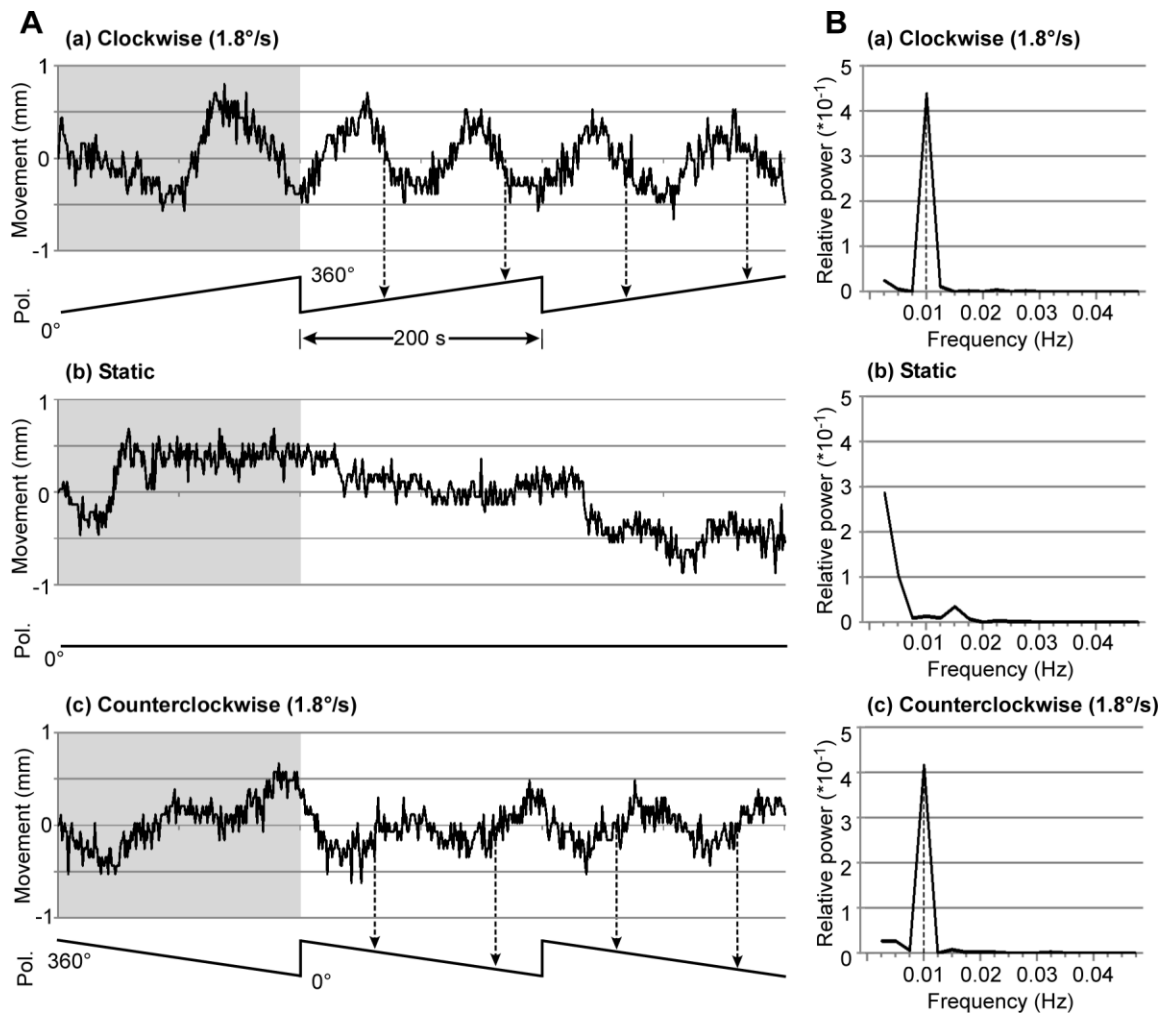


Fig. 2. A bee's abdominal movement under the polarized light stimulus. Trajectories of the abdominal tip (**A**) and the power spectrum (**B**) under the clockwise (1.8° s^{-1} ; **a**), static (**b**), and counterclockwise (1.8° s^{-1} ; **c**) stimulus. The lower trace in each trajectory (Pol.) indicates the e-vector orientation of the polarizer with respect to the bee's body axis, and preferred e-vector orientations of the bee are indicated by dashed arrows (126° and 112° for clockwise and counterclockwise stimulus, respectively). Under rotating e-vector (**a** and **c**), the abdomen showed periodical movements from side to side. Dashed lines indicate the peaks at the stimulus rotation frequency (0.01 Hz). The first 200 s of the trajectory (gray) was not used for FFT analysis.

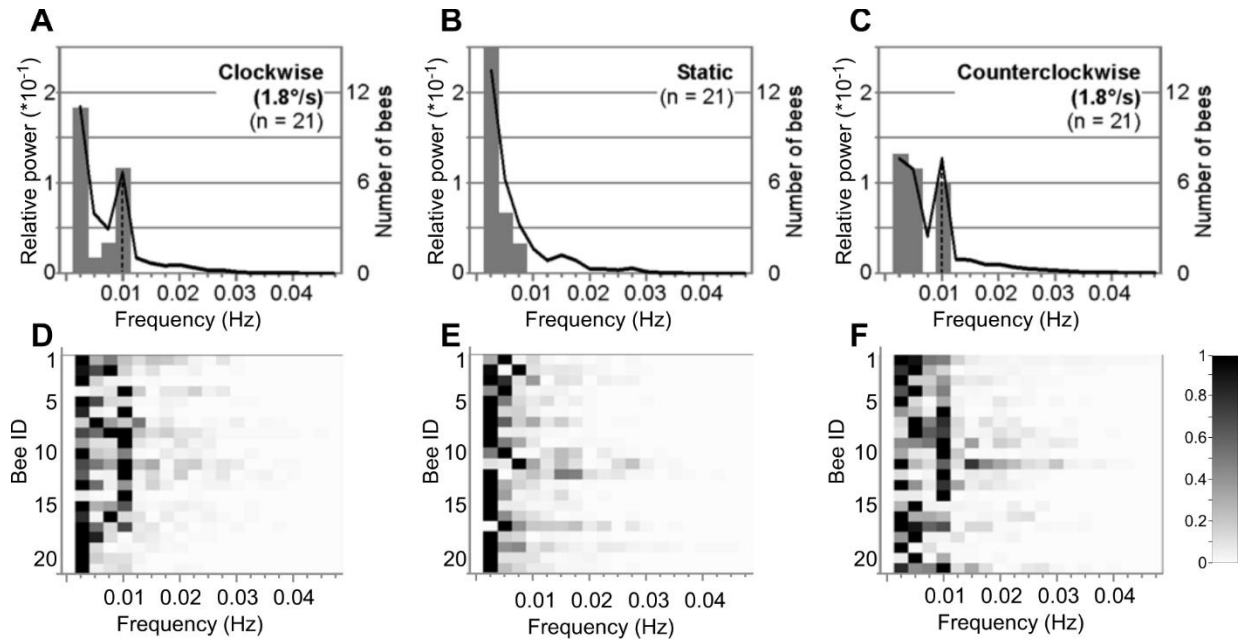


Fig. 3. Power spectra of the abdominal movements under the polarized light stimulus. A-C. Averaged power spectra (black line) and histograms of the maximum peak in each power spectrum (gray bars) are shown ($N = 21$). Dashed lines indicate the peaks at the stimulus rotation frequency (0.01 Hz). **D-F.** Heat maps of power spectra (normalized by the maximum power) of all experimental bees shown in A-C. ($N = 21$). **A, D:** clockwise stimulus (1.8° s^{-1}); **B, E:** static stimulus; **C, F:** counterclockwise stimulus (1.8° s^{-1}).

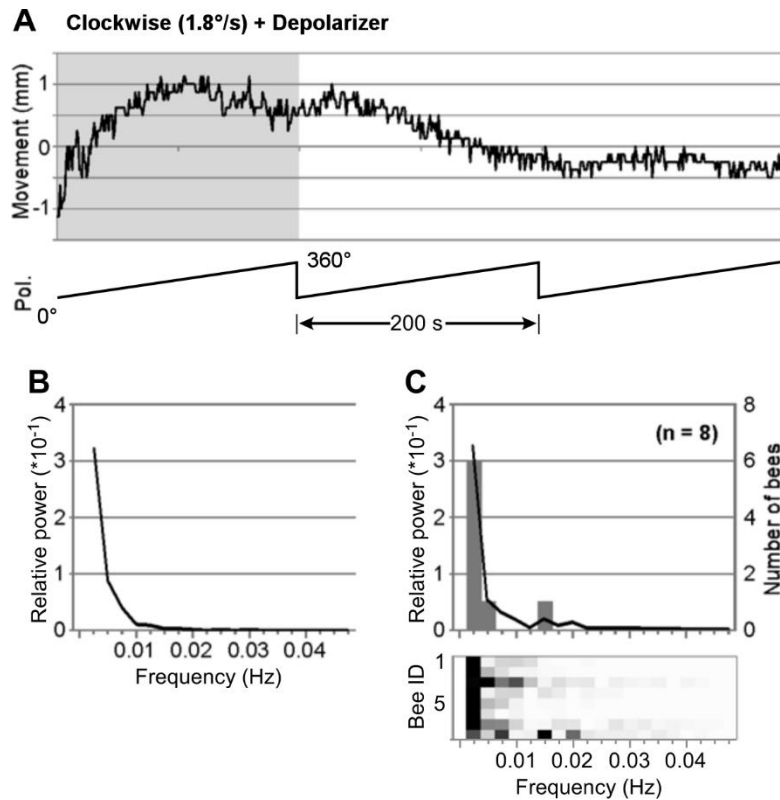


Fig. 4. Abdominal movements under the depolarized light stimulus. **A.** An example of the bee's abdominal trajectory. A UV-transmitted depolarizer was put below the rotating polarizer (1.8° s^{-1}), just above the bee's head such that the size of the light stimulus covered the entire receptive field of the bee's DRA. The lower trace (Pol.) indicates the e-vector orientation of the polarizer with respect to the bee's body axis. The first 200 s of the trajectory (gray) was not used for FFT analysis. **B.** The power spectrum of the abdominal trajectory shown in A. **C.** Upper: averaged power spectrum (black line) and the histogram of the maximum peak in each power spectrum (gray bars) are shown ($N = 8$). Lower: heat maps of power spectra (normalized by the maximum power) of all experimental bees ($N = 8$).

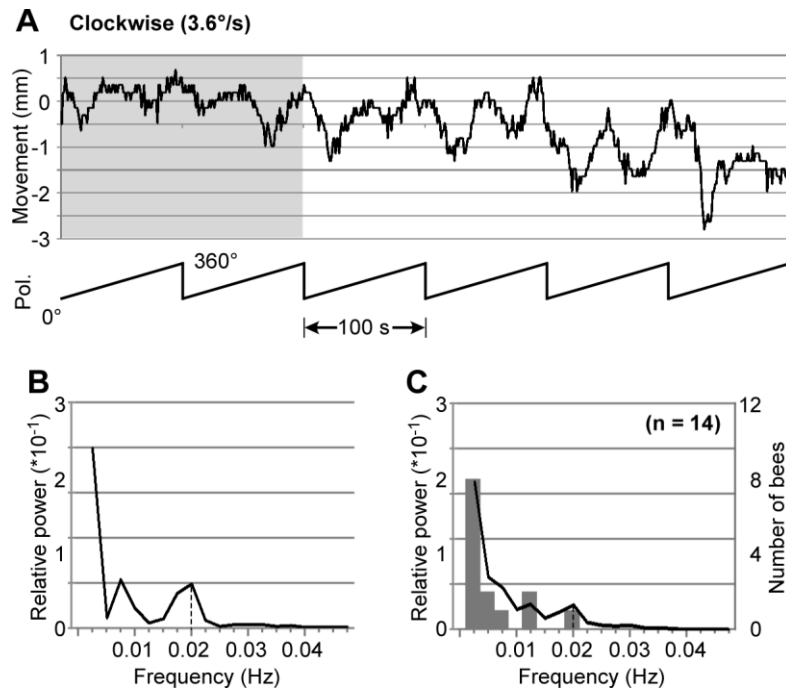


Fig. 5. Abdominal movements under the rotating polarized light stimulus (3.6° s^{-1}). **A.** An example of a bee's abdominal trajectory. The lower trace (Pol.) indicates the e-vector orientation of the polarizer with respect to the bee's body axis. The first 200 s of the trajectory (gray) was not used for FFT analysis. **B.** The power spectrum of the abdominal trajectory shown in A. **C.** Averaged power spectrum (black line) and the histogram of the maximum peak in each power spectrum (gray bars) are shown ($N = 14$). Dashed lines indicate the peaks at the stimulus rotation frequency (0.02 Hz).

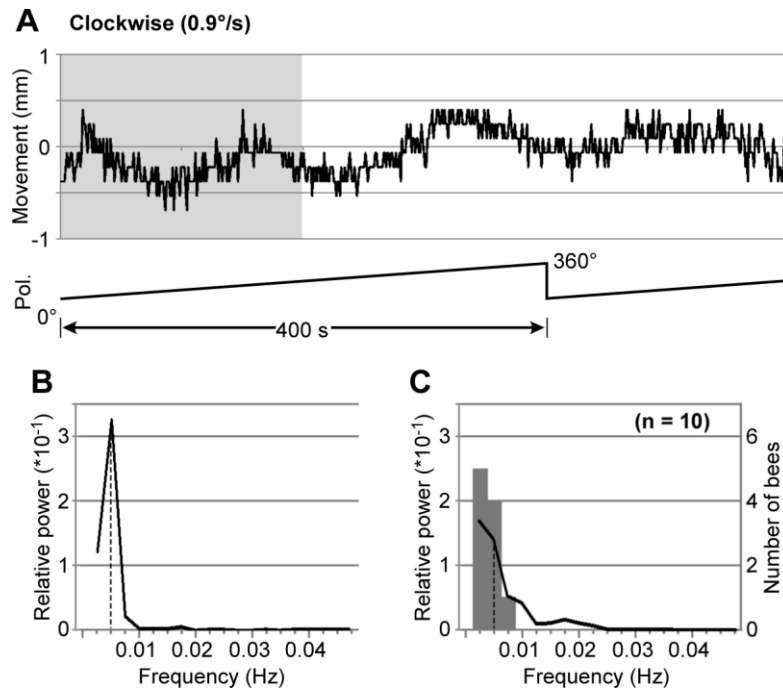


Fig. 6. Abdominal movements under the rotating polarized light stimulus (0.9° s^{-1}). **A.** An example of a bee's abdominal trajectory. The lower trace (Pol.) indicates the e-vector orientation of the polarizer with respect to the bee's body axis. The first 200 s of the trajectory (gray) was not used for FFT analysis. **B.** The power spectrum of the abdominal trajectory shown in A. **C.** Averaged power spectrum (black line) and the histogram of the maximum peak in each power spectrum (gray bars) are shown ($N = 10$). Dashed lines indicate the peaks at the stimulus rotation frequency (0.005 Hz).

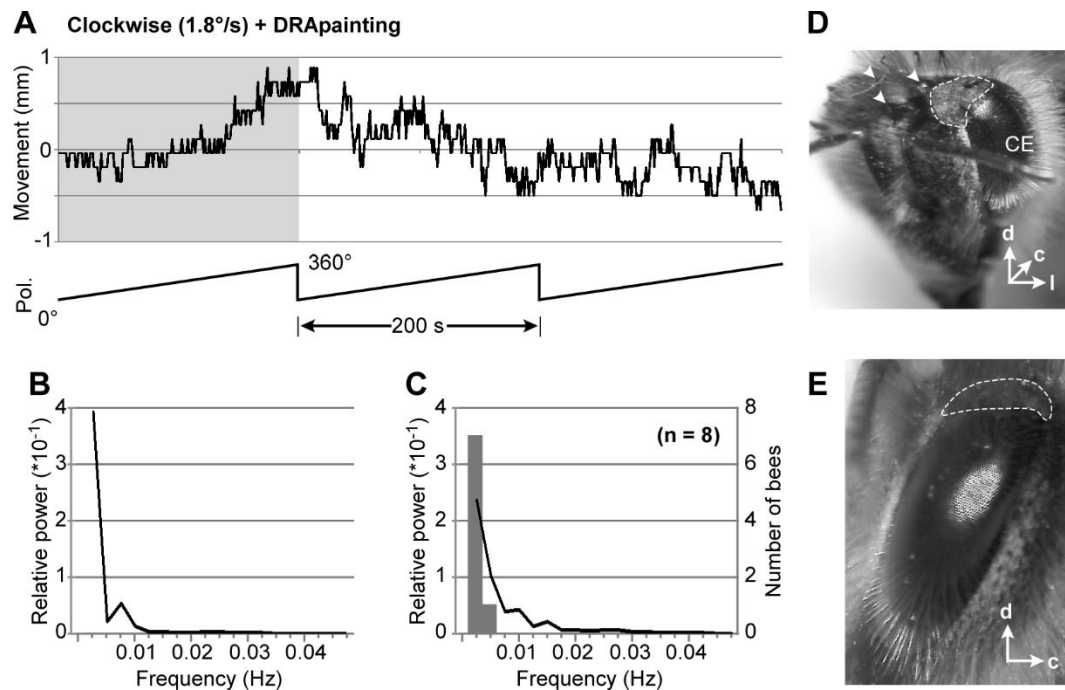


Fig. 7. Abdominal movements of the DRA-covered bees under the rotating polarized light stimulus (1.8° s^{-1}). **A.** An example of a bee's abdominal trajectory. The lower trace (Pol.) indicates the e-vector orientation of the polarizer with respect to the bee's body axis. The first 200 s of the trajectory (gray) was not used for FFT analysis. **B.** The power spectrum of the abdominal trajectory shown in A. **C.** Averaged power spectrum (black line) and the histogram of the maximum peak in each power spectrum (gray bars) are shown ($N = 8$). **D.** Head of the bee after its DRAs were painted. The area surrounded by the dashed line was painted. Arrow heads indicate the ocelli. CE: compound eye. **E.** Lateral view of the compound eye of the bee shown in D.

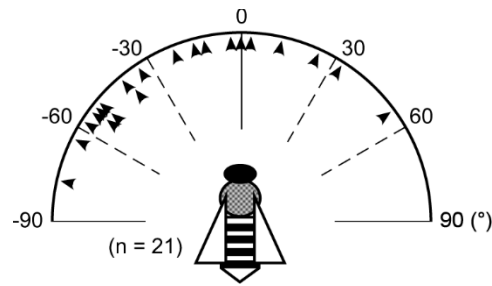


Fig. 8. Preferred e-vector orientations (PEOs) of the bees caught at the hive entrance. PEOs of the bees that showed polarotaxis under clockwise rotating stimulus ($1.8^{\circ} \text{ s}^{-1}$) with respect to the bee's body axis ($N = 21$). The distribution was not significantly random ($p = 0.01$, Rayleigh test).

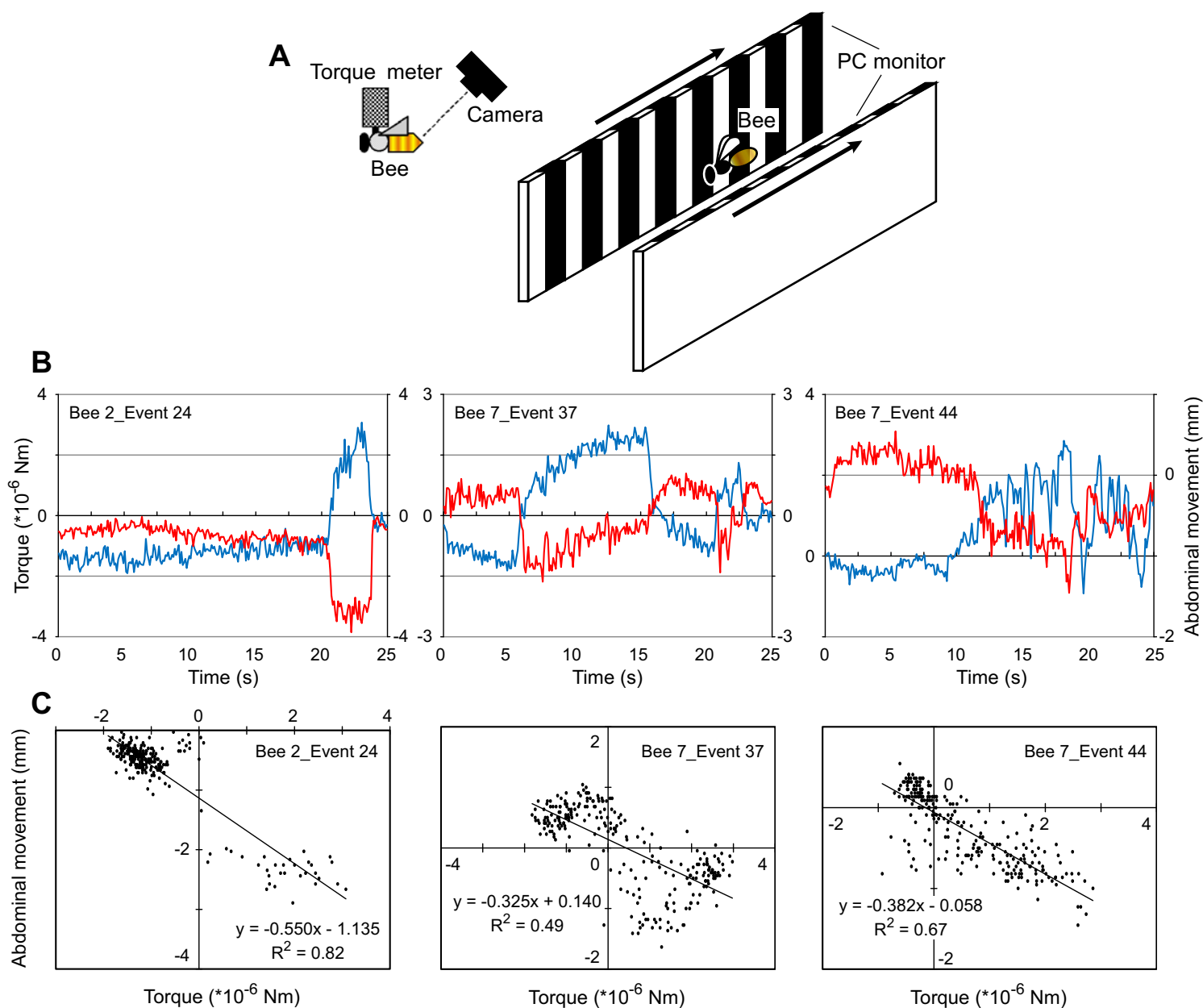


Fig. S1 Correlations of the torque with the abdominal tip. **A.** Experimental setup. **B.** Time traces of the torque (blue) and horizontal movement of the abdominal tip (red). **C.** Scatter plots of torque and the position of the abdominal tip. Sixty-three out of 73 flights showed a negative correlation coefficient.

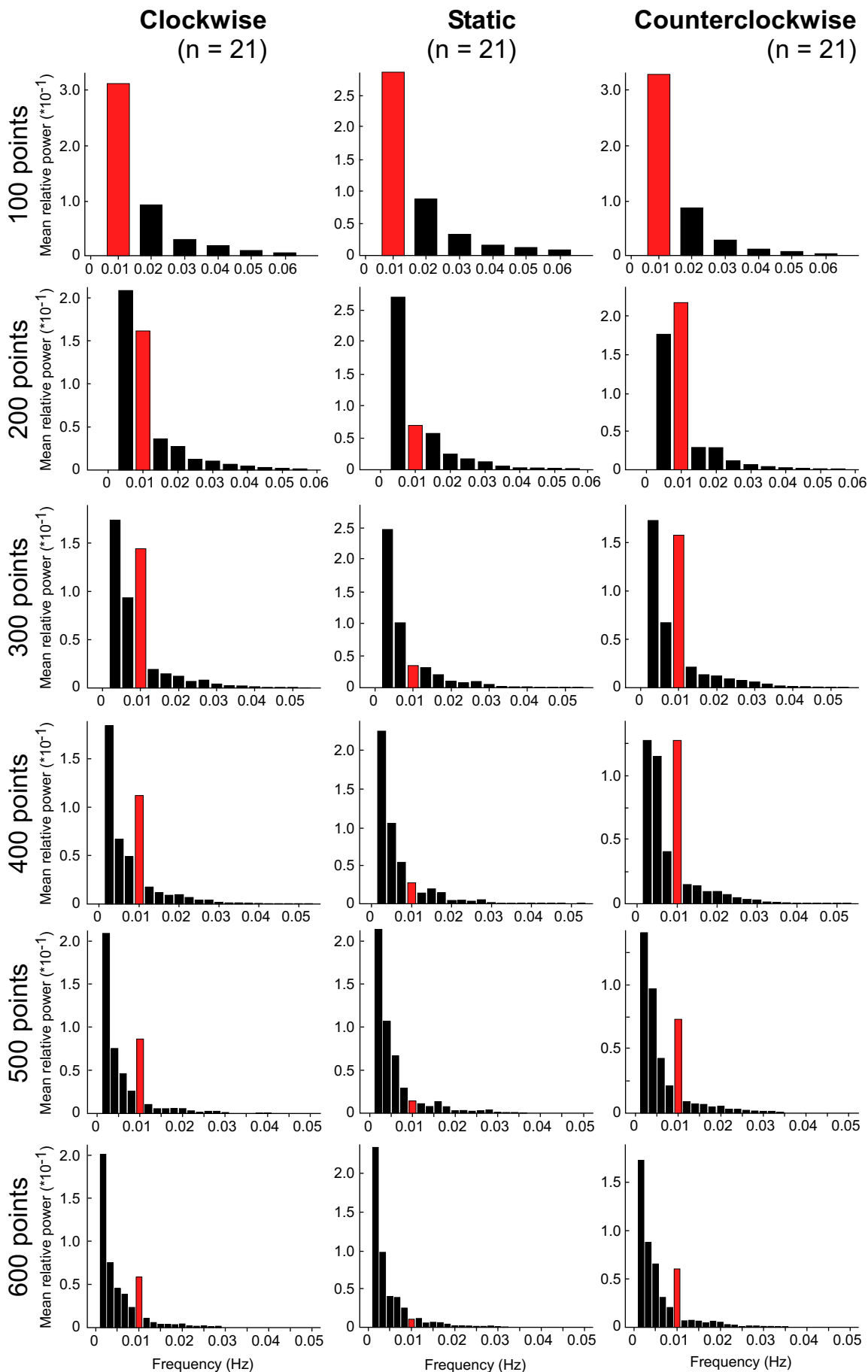


Fig. S2 Power spectra obtained from different data lengths. Mean relative PSs were calculated from 21 bees each of which were used for all three simulation conditions: clockwise rotation, counter clockwise rotation, and static condition. 100, 200, 300, 400, 500, and 600 points ($1 \text{ point} \cdot \text{sec}^{-1}$) from the end of measuring were extracted for calculating relative PSs. Because the frequency resolution depends on the data length mathematically, the lowest frequency component (this is defined as a fundamental frequency mathematically) is different among different data-length groups, e.g. 0.01 Hz for 100-points group and 0.002 Hz for 500-points group. The lowest frequency component is large in all cases. On the contrast, 0.01 Hz components (red bars) were large data-length independently only when the polarized filter was rotated. Note that the fundamental frequency was different among data-length.

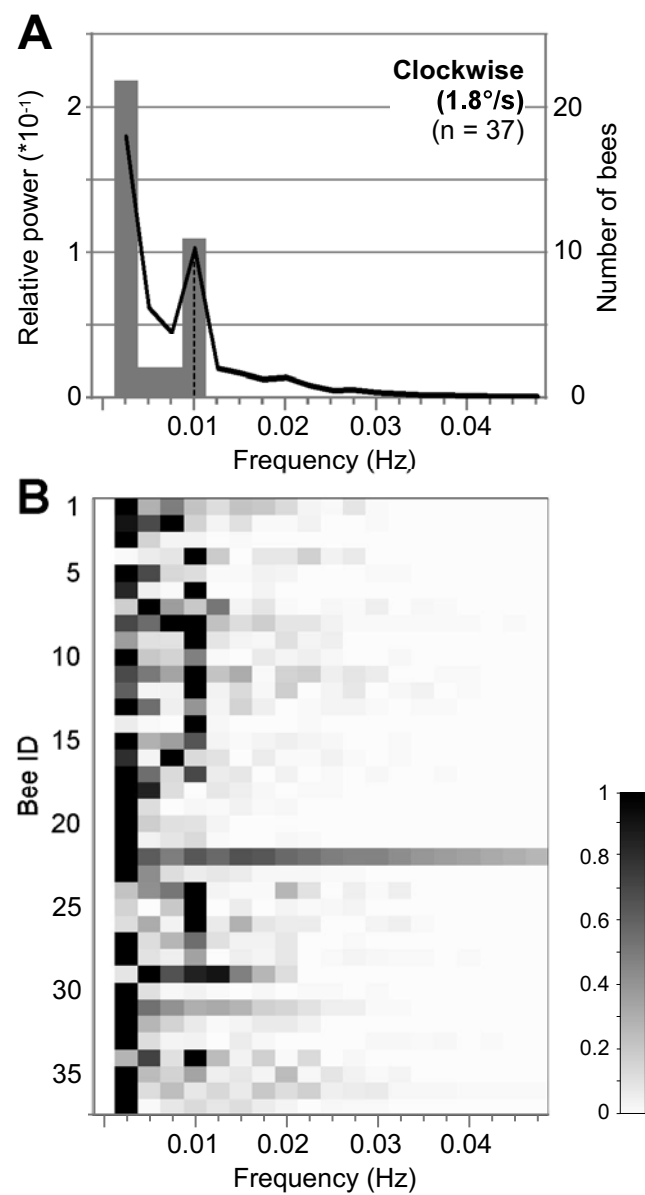


Fig. S3 Power spectra of the abdominal movements under the clockwise (1.8 ° s⁻¹) stimulus. A. An averaged power spectrum (black line) and a histogram of the maximum peak in each power spectrum (gray bars) are shown (N = 37). Dashed lines indicate the peaks at the stimulus rotation frequency (0.01 Hz). **B.** Heat maps of power spectra (normalized by the maximum power) of all experimental bees shown in A (N = 37). Note that the 21 of 37 bees were the same individuals shown in Fig. 3.

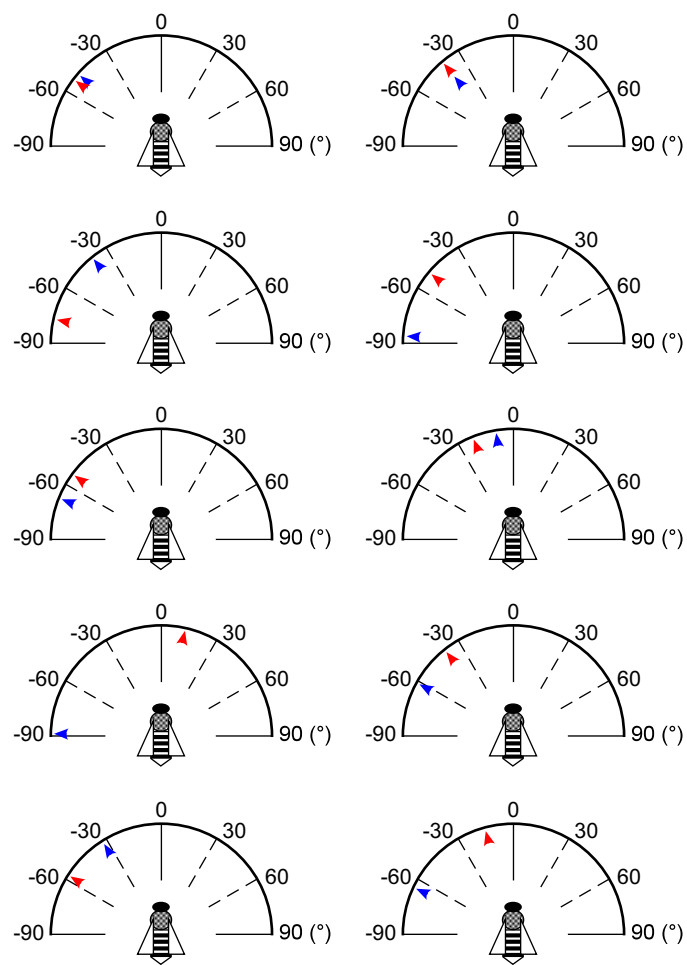


Fig. S4 Preferred e-vector orientations (PEOs) under the clockwise and counterclockwise stimulus. PEOs of each bee that exhibited polarotaxis both under clockwise (red) and counterclockwise (blue) rotating stimuli ($1.8^{\circ} \text{ s}^{-1}$) are shown with respect to the bee's body axis ($N = 10$, see also Fig. 3).

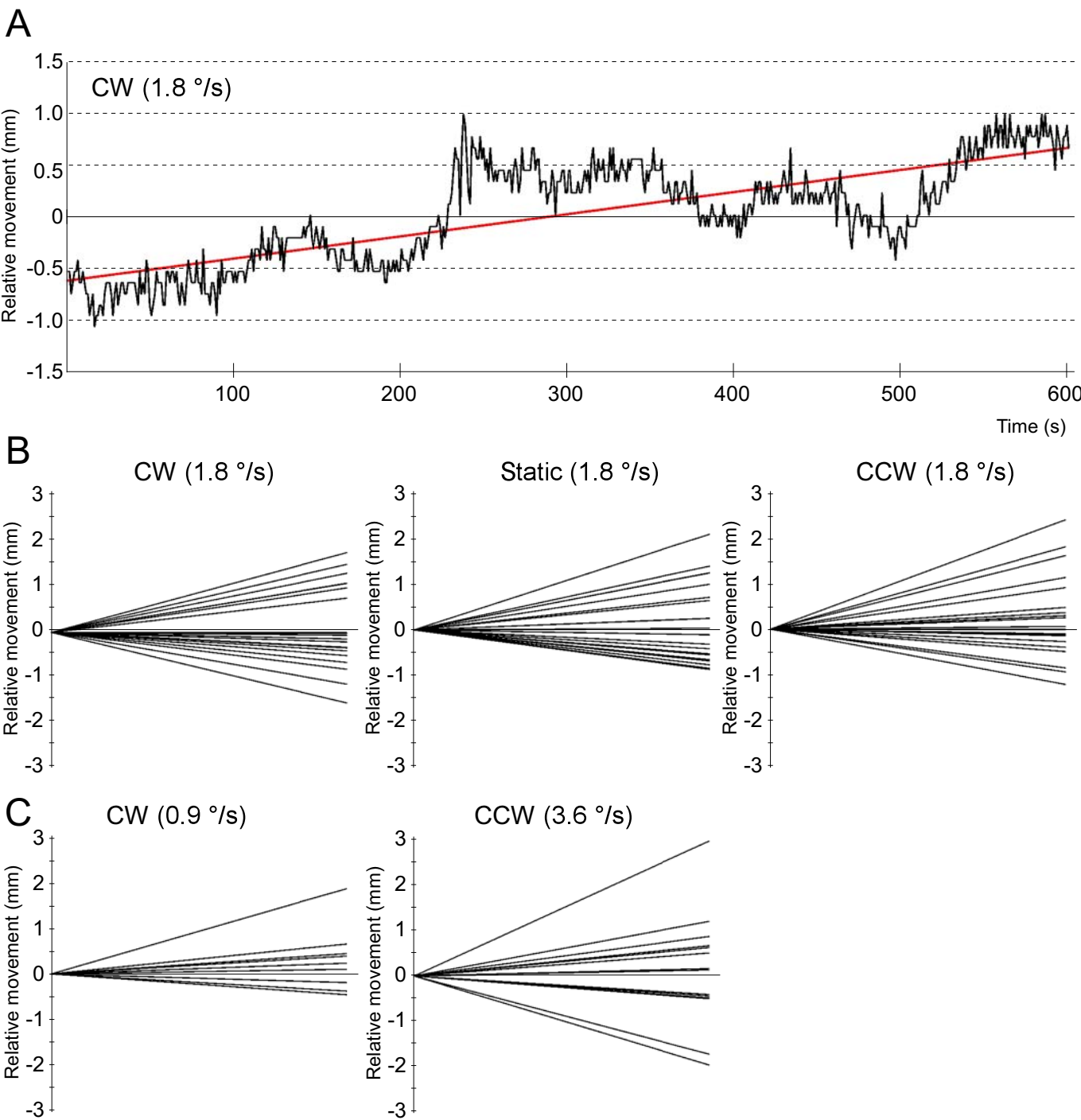


Fig. S5 Trends of steering directions. The trend of the response trajectory was obtained as the slope of a line calculated by linear fitting of the trajectory using the least squares. To compare the trends among individuals (B, C), starting points of the slopes were set at zero. **A.** An example of trajectory of the abdominal tip under the clockwise ($1.8^{\circ} s^{-1}$) stimulus. The red line indicate the trend of this behavioral response. **B.** Trends of 21 bees for clockwise (CW), static, and counterclockwise (CCW) 600-second stimulus at speed of $1.8^{\circ} s^{-1}$. **C.** Trends of another bee groups for the slow and fast speed under the 600-second clockwise stimulus ($N = 10$ and 14 for $0.9^{\circ} s^{-1}$ and $3.6^{\circ} s^{-1}$ stimulus, respectively).

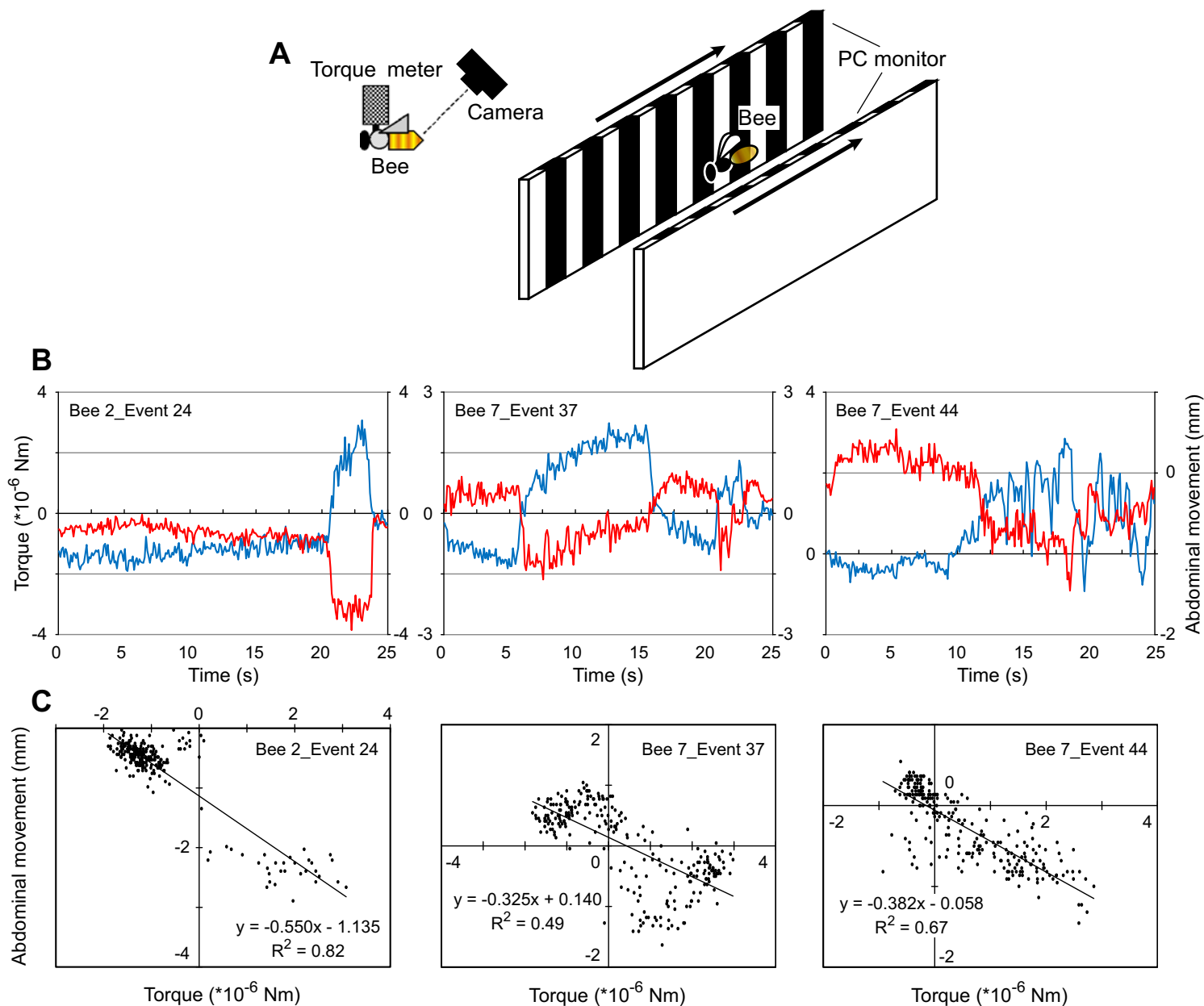


Fig. S1 Correlations of the torque with the abdominal tip. **A.** Experimental setup. **B.** Time traces of the torque (blue) and horizontal movement of the abdominal tip (red). **C.** Scatter plots of torque and the position of the abdominal tip. Sixty-three out of 73 flights showed a negative correlation coefficient.

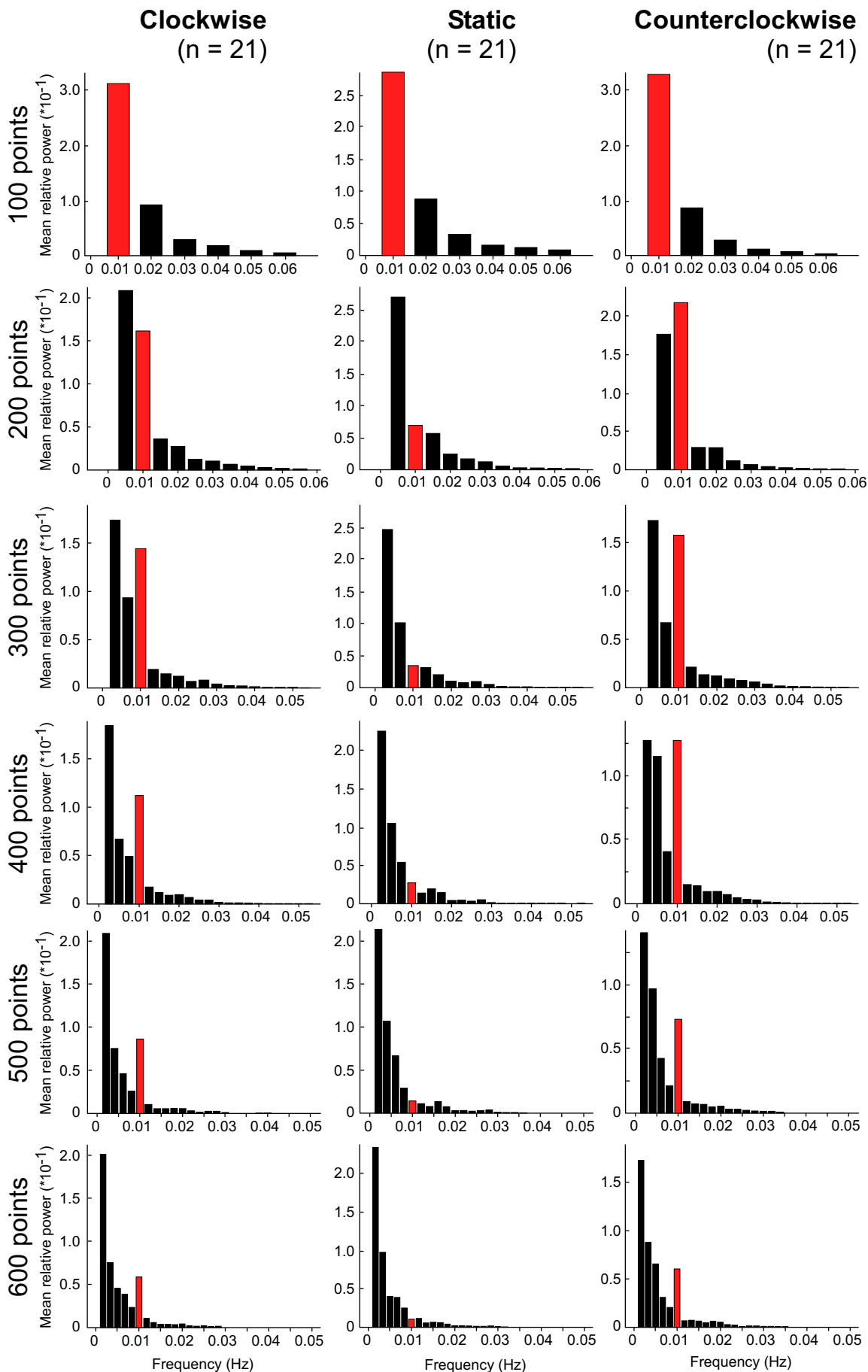


Fig. S2 Power spectra obtained from different data lengths. Mean relative PSs were calculated from 21 bees each of which were used for all three simulation conditions: clockwise rotation, counter clockwise rotation, and static condition. 100, 200, 300, 400, 500, and 600 points ($1 \text{ point} \cdot \text{sec}^{-1}$) from the end of measuring were extracted for calculating relative PSs. Because the frequency resolution depends on the data length mathematically, the lowest frequency component (this is defined as a fundamental frequency mathematically) is different among different data-length groups, e.g. 0.01 Hz for 100-points group and 0.002 Hz for 500-points group. The lowest frequency component is large in all cases. On the contrast, 0.01 Hz components (red bars) were large data-length independently only when the polarized filter was rotated. Note that the fundamental frequency was different among data-length.

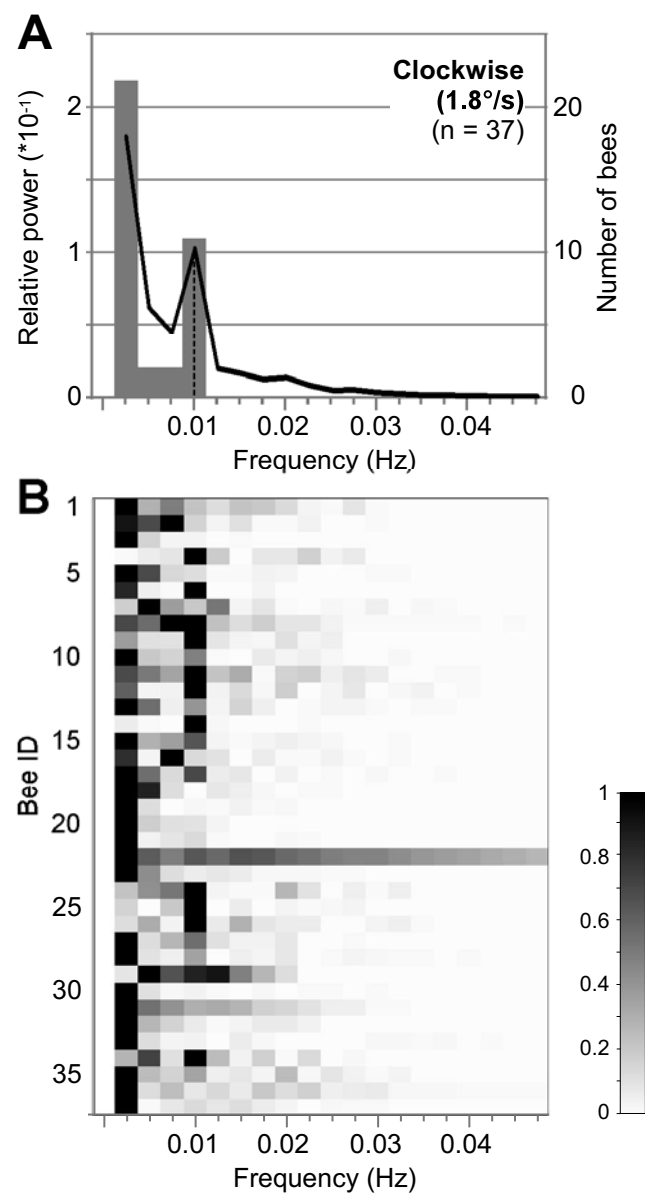


Fig. S3 Power spectra of the abdominal movements under the clockwise (1.8 ° s⁻¹) stimulus. A. An averaged power spectrum (black line) and a histogram of the maximum peak in each power spectrum (gray bars) are shown (N = 37). Dashed lines indicate the peaks at the stimulus rotation frequency (0.01 Hz). **B.** Heat maps of power spectra (normalized by the maximum power) of all experimental bees shown in A (N = 37). Note that the 21 of 37 bees were the same individuals shown in Fig. 3.

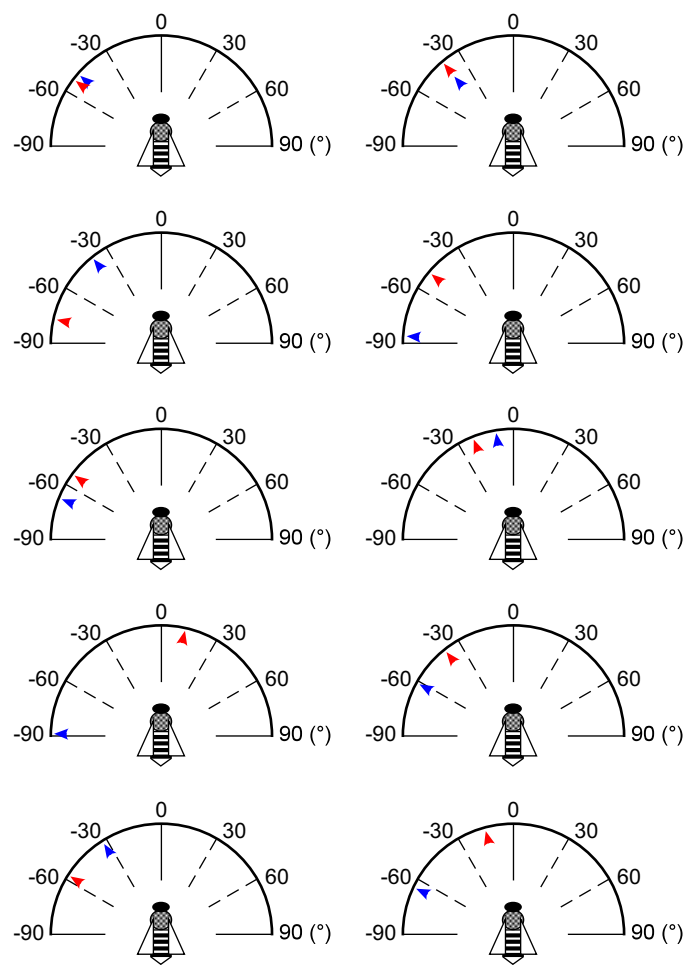


Fig. S4 Preferred e-vector orientations (PEOs) under the clockwise and counterclockwise stimulus. PEOs of each bee that exhibited polarotaxis both under clockwise (red) and counterclockwise (blue) rotating stimuli ($1.8^{\circ} \text{ s}^{-1}$) are shown with respect to the bee's body axis ($N = 10$, see also Fig. 3).

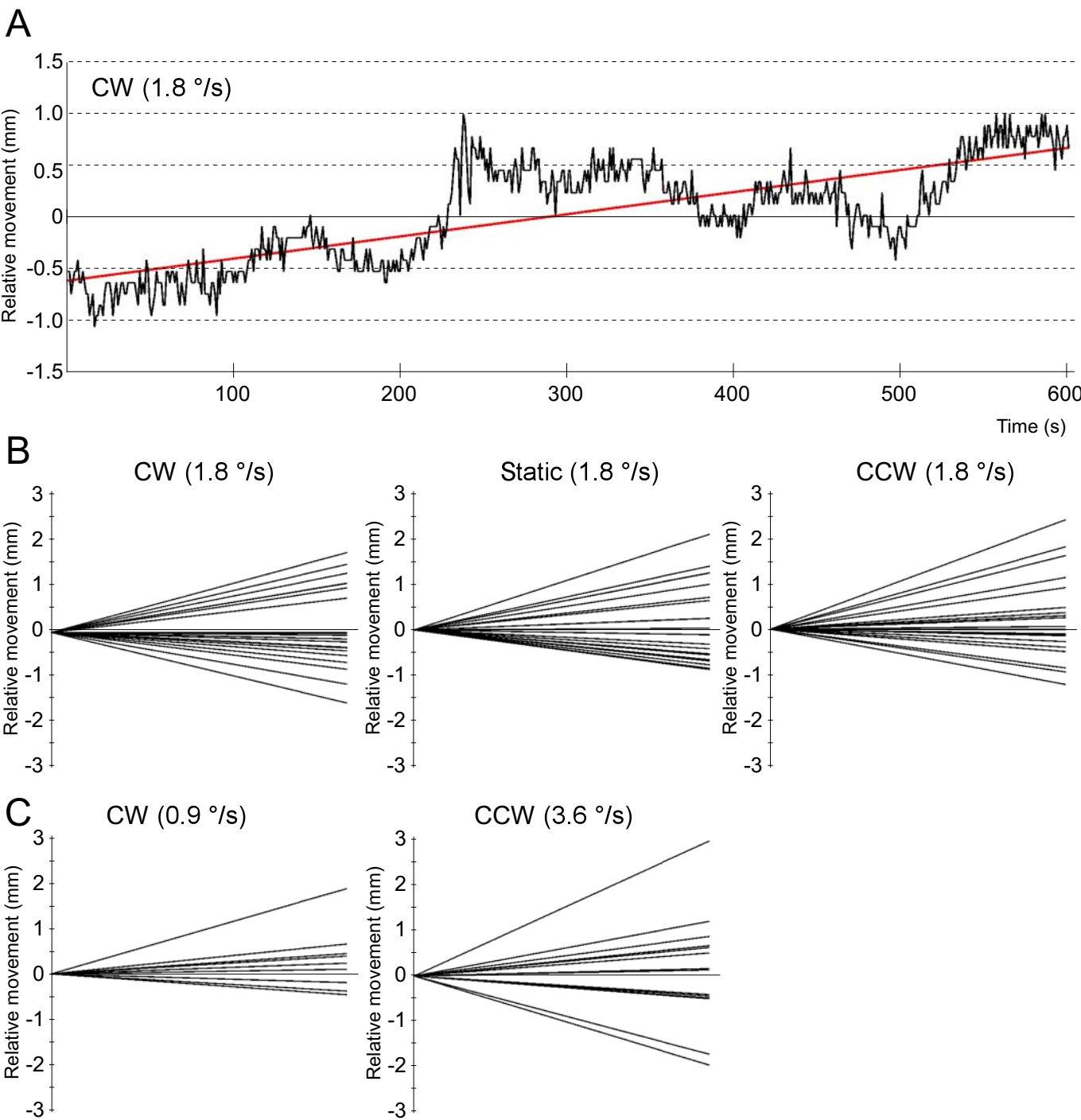


Fig. S5 Trends of steering directions. The trend of the response trajectory was obtained as the slope of a line calculated by linear fitting of the trajectory using the least squares. To compare the trends among individuals (B, C), starting points of the slopes were set at zero. **A.** An example of trajectory of the abdominal tip under the clockwise ($1.8^{\circ} \text{ s}^{-1}$) stimulus. The red line indicate the trend of this behavioral response. **B.** Trends of 21 bees for clockwise (CW), static, and counterclockwise (CCW) 600-second stimulus at speed of $1.8^{\circ} \text{ s}^{-1}$. **C.** Trends of another bee groups for the slow and fast speed under the 600-second clockwise stimulus ($N = 10$ and 14 for $0.9^{\circ} \text{ s}^{-1}$ and $3.6^{\circ} \text{ s}^{-1}$ stimulus, respectively).